Combined Experimental and Computer Simulation Study of the Kinetics of Solute Release from a Relaxing Swellable Polymer Matrix. II. Release of an Osmotically Active Solute

K. G. Papadokostaki

Institute of Physical Chemistry, Demokritos National Research Center, 15310 Aghia Paraskevi, Athens, Greece

Received 4 August 2003; accepted 19 September 2003

ABSTRACT: The performance of a model monolithic controlled release device, consisting of a swellable polymeric matrix subject to structural relaxation (cellulose acetate), loaded with a simple osmotically active solute (NaCl) and activated by the ingress of solvent (water), was studied experimentally and by computer simulation. The former study involved detailed monitoring of the kinetics of both solute release and solvent absorption (followed in due course by desorption of osmotically imbibed excess solvent). The computer simulation study was based on extensive previous modeling work. Values of the relevant input model parameters were derived from independent experimental measurements of the sorption and diffusion properties of solvent (cf. Part I) and solute (reported in the present article). The resulting simulation was highly successful, considering that it proved possible to simulate closely and consistently the kinetics of both solute release (over practically the whole experimental range) and concurrent solvent absorption (including correct prediction of the magnitude of the osmotically induced excess swelling of the polymeric matrix). Simulation of the final desorption of osmotically imbibed water was facilitated by the realization that this process actually reflects the kinetics of a long-term deswelling relaxation of the polymer structure back to the state of normal hydration, the rate of which could be measured to a good approximation on the pure deswelling polymer. The results presented here are of obvious practical significance in relation to progress toward computer-assisted design of monolithic controlled release devices exhibiting relatively complex kinetic behavior. They should also prove useful by calling attention to an important caveat when desorption into water is used as a method for the straightforward determination of solute diffusivity in hydrated polymers, in cases of osmotically active solutes diffusing in nonhydrophilic polymers.
 J Appl Polym Sci 92: 2468–2479, 2004

Key words: diffusion; polymer relaxation; ionic sorption; monolithic controlled release devices; computer modeling

INTRODUCTION

In the present article, we report an experimental study of the release of an osmotically active solute (NaCl) from cellulose acetate (CA) films into an aqueous phase, with simultaneous monitoring of concomitant variation of the water content of the matrix. We then proceed to simulate on the computer the combined kinetic behavior of solvent and solute. This simulation is based on a previously developed modeling approach to solute release from relaxing glassy polymer matrices,[1] complemented by (1) information gained from our preceding study of non-Fickian liquid water uptake by CA films[2] and (2) subsidiary solute sorption and diffusion measurements undertaken here, for the independent determination of model parameters.

Correspondence to: K. G. Papadokostaki (kpapadok@chem.demokritos.gr).

Contract grant sponsor: General Secretariat for Research and Technology, Greece and European Union.

Journal of Applied Polymer Science, Vol. 92, 2468–2479 (2004)

The notation of refs. 1 and 2 is maintained, except for the fact that it was found more convenient here to use a different mode of normalization of solute-related parameters [see eq. (11) below].

THEORETICAL MODEL

The full model of ref. 1, incorporating the extension presented in Part I,[2] is as follows.

The transport of solvent (subscript W) and solute (subscript N), contained in a monolith in the form of a swellable thin film (of thickness $2l$), preequilibrated with solvent at activity $a_W = a_{W0}$ and exposed to bulk solvent ($a_W = 1$) at time $t \geq 0$, is described by[1,3]

$$\frac{\partial C_W}{\partial t} = \frac{\partial}{\partial x}\left(D_W S_W \frac{\partial a_W}{\partial x}\right); \quad \frac{\partial C_N}{\partial t} = \frac{\partial}{\partial x}\left(D_N S_N \frac{\partial a_N}{\partial x}\right) \tag{1a, b}$$

with boundary conditions

$$a_W = a_{W0} \quad (C_W = C_{W0}); \quad a_N = a_{N0} \quad (C_N = C_{N0}); \quad \text{at} \quad t = 0, \quad 0 < x \leq l \tag{2a}$$

$$a_W = 1; \quad a_N = 0 \quad (C_N = 0); \quad \text{at} \quad t \geq 0, \quad x = 0 \quad (2b)$$

$$\partial a_W/\partial x = \partial a_N/\partial x = 0; \quad \text{at} \quad t \geq 0, \quad x = l \quad (2c)$$

In eqs. (1) and (2), $0 \leq x \leq l$ represents distance across one-half of the film (measured in units referred to the unswollen matrix), with $x = 0$ at the exposed surface; C, a, S, and D represent concentration (measured in mole or gram per unit volume or mass of unswollen polymer), activity, solubility coefficient, and (thermodynamic) diffusion coefficient, respectively, of the relevant species in the matrix.

Solvent parameters

The activity of solvent (water) a_W, at given x, t, is defined to be equal to the relative vapor pressure (relative humidity) which would be at equilibrium with C_W, at that x, t (with due vapor nonideality correction if desired), bearing in mind that the relevant a_W value will also depend on (1) the value of C_N, at the given x, t, if the solute is osmotically active,[1,3] and (2) the state of relaxation of the polymer.[1,2] These effects are taken into account by defining absorption isotherms for the fully relaxed and unrelaxed polymer matrix,[1,2] augmented[1,3] with a suitable dependence on C_N. Thus, eqs. (2), (2a), and (3) of Part I[2] become, respectively,

$$C_{WF} = F_F(a_W)f_N(C_N) = [F_F(a_{W0}) + f_F(\delta a_W)]f_N(C_N) \quad (3a, b)$$

$$C_{WI} = [F_F(a_{W0}) + f_I(\delta a_W)]f_N(C_N) \quad (4)$$

where $f_N(C_N)$ may be any convenient function which can adequately represent the behavior of the particular system of interest, subject to the condition $f_N(C_N = 0) = 1$. The linear expression

$$f_N(C_N) = 1 + K_{W3}C_N \quad (5)$$

was chosen for the theoretical investigations previously reported[1,3] as the simplest function fulfilling the aforementioned condition (while Polishchuk et al.[4] opted for an exponential dependence). For the same reasons, a unique K_{W3} value was specified[1] for eqs. (3) and (4). This practice is followed here also in the case of the incremental absorption isotherms associated with relaxation (governed by relaxation frequencies β_{Wi}) defined by eq. (5) of Part I,[2] which becomes

$$\delta C_{WFi} = f_i(\delta a_W)f_N(C_N) \quad (6)$$

On the other hand, eq. (9) of Part I[2] (used to calculate, at a given location x, the change in activity Δa_W associated with the change in concentration ΔC_W, over a time interval Δt) becomes

$$\frac{\partial C_W}{\partial t} = \frac{\partial C_{WI}}{\partial a_W}\frac{\partial a_W}{\partial t} + \sum_{i=1}^{N_R} \beta_{Wi}(\delta C_{WFi} - \delta C_{Wi}) + \frac{\partial C_{WI}}{\partial C_N}\frac{\partial C_N}{\partial t} \quad (7)$$

where the third term has been added[1] to account for the osmotic effect of the concomitant change in solute concentration ΔC_N [which is given by eq. (1b)].

The solubility coefficient is defined as $S_W = C_W/a_W$ and is thus dependent on both solute concentration and the state of relaxation of the polymeric matrix.

Our previous practice[1–3] of using constant effective values of D_W and β_{Wi} is continued here (and is justified *a posteriori* by the results achieved; see below).

Solute parameters

At any x, t in the hydrated matrix, the solute may exist in mobile (dissolved, concentration C_{NS}) and immobile (finely dispersed, concentration C_N–C_{NS}) forms, at equilibrium with each other. The solubility coefficient is defined[1,3] as $S_N = C_{NS}/a_N$. The activity a_N is, in turn, defined[1,3] as $a_N = c_{NS}/c^0_{NS}$, where c_{NS} is the concentration of an aqueous solution of the solute, which would be at equilibrium with C_{NS}, and c^0_{NS} represents the saturation value of c_{NS} (both c_{NS} and c^0_{NS} are subject to nonideality corrections if desired). C_{NS} is an increasing function of C_W. We may write[1,3]

$$S_N = \frac{C_{NS}}{a_N} = k_s C_W \bar{V}_W c^0_{NS} = K_N C_W \quad (8)$$

where $\bar{V}_W$ is the molar (or specific) volume of water; C_W, C_{NS} are expressed in mol (or g) per unit mass (or volume) of the dry film; and (as discussed in more detail below; cf. also ref. 3) the magnitude of the distribution coefficient k_s is determined by the relative strength of polymer–solute and solvent–solute interactions and may vary with C_W. The dissolved solute attains saturation at $a_N = 1$. Thus, by eq. (8), S_N represents the saturation value of C_{NS} at given C_W. Hence, if $C_N > S_N$, dispersed solute exists and is assigned concentration C_N–S_N and activity $a_N = 1$. Accordingly, at any x, t during the diffusion process, the value of S_N may be determined from the local C_W via eq. (8) and the corresponding local C_{NS} and a_N calculated from

$$C_{NS} = C_N, \quad a_N = C_{NS}/S_N; \quad \text{if} \quad C_N < S_N \quad (9a)$$

$$C_{NS} = S_N, \quad a_N = 1; \quad \text{if} \quad C_N \geq S_N \quad (9b)$$

Under the specific experimental conditions used in the present work, $a_N < 1$. Thus, eq. (9a) may be expected to hold at all x, t.

The dependence of the diffusion coefficient of solute on the degree of hydration of the matrix may, following Yasuda et al.,[5] be described by[1,3]

$$D_N = D_{NS}\exp\left(-\frac{B_{N1}}{B_{N2} + C_W}\right) \quad (10)$$

where D_{NS} is the diffusion coefficient in aqueous solution and B_{N1} and B_{N2} are positive constants. The value of D_N in the fully hydrated ($C_W = C_W^0$), solute-free matrix, namely $D_{NE} = D_N$ ($C_W = C_W^0$), offers perhaps the simplest and most convenient way of characterizing the solute diffusivity properties of this system.

Method of solution

The model variables and parameters were expressed in dimensionless form (denoted by bold type) as follows:

$$\mathbf{x} = x/l, \quad \mathbf{t} = D_W t/l^2, \quad \mathbf{C_W} = C_W/C_W^0,$$
$$\mathbf{C_N} = C_N/C_W^0, \quad \mathbf{C_{NS}} = C_{NS}/C_W^0, \quad \mathbf{S_N} = S_N/C_W^0,$$
$$\mathbf{S_W} = S_W/C_W^0, \quad \boldsymbol{\beta_W} = l^2\beta_W/D_W, \quad \mathbf{K_{W1}} = K_{W1}/C_W^0,$$
$$\mathbf{K_{W2}} = K_{W2}/C_W^0, \quad \mathbf{K_{WS}} = K_{WS}/C_W^0, \quad \mathbf{K_{W3}} = K_{W3}C_W^0,$$
$$\mathbf{D_N} = D_N/D_W, \quad \mathbf{D_{NS}} = D_{NS}/D_W, \quad \mathbf{B_{N1}} = B_{N1}/C_W^0,$$
$$\mathbf{B_{N2}} = B_{N2}/C_W^0 \quad (11)$$

It follows that $\mathbf{C_W^0} = 1$, $\mathbf{S_W}$ ($a_W = 1$, $C_N = 0$) $= 1$, $\mathbf{S_N}$ ($C_W = C_W^0$) $= K_N$, $\mathbf{D_W} = 1$.

The solution of eqs. (1a, b) and (7), using eqs. (2), was effected by dividing the half-space $0 \le \mathbf{x} \le 1$ into N intervals and applying an explicit finite difference method of numerical solution.[1] Starting at $\mathbf{t} = 0$ (eq. 2a), the changes of $\mathbf{C_W}$, a_W, and $\mathbf{C_N}$ at positions $\mathbf{x_n} = n/N$ ($n = 0, 1, 2, \ldots, N$) were calculated, over successive small time intervals $\Delta\mathbf{t}$, from the numerical approximations to eqs. (1a, b) and (7), with the aid of relations (3)–(6). The corresponding changes in a_N were deduced at each step from eqs. (8) and (9a). Care was taken to adjust $\Delta\mathbf{t}$ periodically, depending on the value of $\Delta\mathbf{x} = 1/N$ (=0.05 usually) employed and the maximum value $\mathbf{D}_{\max}$ among the current range of $\mathbf{D_W}$ and $\mathbf{D_N}$ values, to keep within the convergence condition of $\Delta\mathbf{t} \le \Delta\mathbf{x}^2/2\mathbf{D}_{\max}$ with reasonable economy of computation. From the resulting diffusion profiles $\mathbf{C_W}(\mathbf{x}, \mathbf{t})$ and $\mathbf{C_N}(\mathbf{x}, \mathbf{t})$, the total fractional solute loss $M_{Nt}/M_{N\infty}$ (where M_{Nt}, $M_{N\infty}$ represent amount eluted at t and $t \to \infty$, respectively) and the mean normalized concentration of imbibed water, $\bar{C}_{Wt}/C_W^0$, were derived by Simpson integration.

EXPERIMENTAL

Materials

CA films of normal degree of hydration (C_W^0 = 0.14–0.17 g/g of dry film), prepared from CA powder (type CA-398-30, Eastman Chemicals, Switzerland) as described in Part I,[2] were used. They were normally kept immersed in water until needed. Film thickness was usually ca. 120 μm or, in a few cases, 300 μm NaCl of analytical grade (Riedel de Haen, Germany) was used as solute.

Equilibrium sorption of solute

Wet CA films were blotted and immersed in NaCl solutions, containing 0.05, 0.12, or 0.25 g/cm^3 of solution, thermostated at 25°C, and shaken periodically. The pH of the solution was between 5.8 and 6.3. Equilibration times were much longer than those calculated according to Fick's equation applicable to long times,[6] especially for solutions of 0.25 g/cm^3 (where significant shrinkage of the membrane was observable).

After equilibration, the films were immersed in water very briefly to remove adhering solution and then blotted and weighed in a weighing bottle for the estimation of sorbed water. The amount of sorbed NaCl was estimated conductimetrically by elution in water.

Solute release kinetics

The elution tests were performed by fixing the film sample (preequilibrated with a given salt solution and blotted) to the rod of a stirrer rotating at 200 rpm, in a known volume of distilled water, thermostated at 25°C, and renewed at frequent intervals. The amount of desorbed salt M_{Nt}, as a function of time t, was determined in the eluate by ionic conductivity and frequently checked by atomic absorption analysis for sodium. To avoid any errors in conductivity measurement, due to atmospheric CO_2 dissolved in water, the latter was boiled before use.

For the determination of the water content of the film ($\bar{C}_{Wt}$) during the elution experiment, the latter was briefly interrupted at appropriate intervals and the specimen was blotted and weighed (making allowance for the weight of remaining solute in the film). Monitoring of the water content of the film was usually continued for a long time after complete elution of the solute.

Ionic sorption and diffusion using radiotracers

Film samples (ca. 120-μm-thick) were first equilibrated in a NaCl solution of the desired concentration (0.05, 0.12, or 0.25 g/cm^3), blotted, and reequilibrated in a second NaCl solution of the same concentration

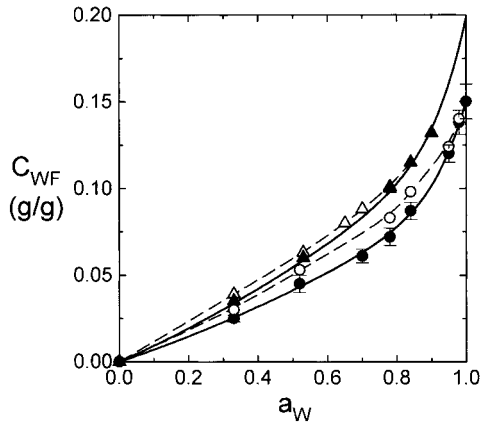

Figure 1 Equilibrium water regain of a CA film loaded with 0.011 g NaCl/g dry film (△, ▲), in comparison with that for neat film (○, ●) by absorption (▲, ●) from, or desorption (△, ○) to, the vapor phase. Solid lines were calculated by eqs. (3) and (12) with the specified parameter values.

containing Na-22 or Cl-36. The films were then very briefly rinsed with an inactive NaCl solution to remove adhering radioactive solution, blotted, and reequilibrated in a third nonradioactive solution of the same concentration and of known weight. The radioactivity of the second and third solutions was measured. Equilibration time was about 1 week in each solution. The kinetics of desorption of the tracer from the film to the third (inactive) solution was also followed (for reasons of safety, a magnetic stirrer was used in this case). Aliquots of the eluting NaCl solution were taken for this purpose at frequent intervals and the amount of desorbed tracer was determined as a function of time. Na-22 was measured by means of a well-type γ-counter and Cl-36 by β-liquid scintillation (2 ml of NaCl solution, diluted if necessary, was added to 15 ml of a scintillation cocktail consisting of 500 ml toluene, 250 ml Triton X-100, 4.125 g PPO, and 0.125 g POPOP), using a Packard TRI-CARB 4430 counter.

Equilibrium water vapor uptake by solute-loaded films

The technique described in Part I[2] was applied to films containing a known quantity of solute. The latter was prepared by equilibrating with a 0.25 g/cm^3 NaCl solution, blotting, and drying by evacuation, at room temperature.

RESULTS AND DISCUSSION

Effect of solute on water vapor sorption isotherm

Figure 1 shows the measured water vapor sorption isotherm at 25°C for film loaded with 0.011 g NaCl/g of dry film (prepared by drying a neat film equilibrated with a 0.25 g/cm^3 NaCl solution, as described in Experimental), in comparison with the corresponding data previously reported for neat films.[2] The amount of water vapor absorbed at relative humidity (RH) 0.83 was, as expected, found to be equal to the water content of neat film at equilibrium with the 0.25 g/cm^3 NaCl aqueous solution, wherein $a_W = 0.83$. As the RH is raised beyond 0.83, the film turns milky (but becomes once again transparent if taken back to RH $\leq$ 0.83), indicating formation of sizeable clusters of water molecules. Beyond this point, the system is effectively supersaturated and eventually water droplets appear on the surface of the film, thus precluding further measurements (cf. analogous behavior of other polymers loaded with NaCl[7]). The difference between NaCl-loaded and neat film isotherms provides a measure of the strength of the osmotic action of the solute, which is embodied in the model parameter K_{W3} defined in eq. (5) (see also below). One may also note that the hysteresis loop in the isotherm of the NaCl-loaded film is very narrow (in keeping with the suggestion[2] that slow structural relaxation in desorption is the primary cause of sorption hysteresis in this system; hence, sorption equilibrium is best considered to be represented by the absorption branch of the experimental isotherm).

According to eqs. (2) and (12) of Part I,[2] the function $F_F(a_W)$ of eq. (3a) is given by

$$F_F(a_W) = K_{W1F}a_W + K_{W2F}a_W^2 + K_{WSF}a_W^s \qquad (12)$$

where, according to the experimental results reported therein, $K_{W1F} = 0.0675$ g/g, $K_{W2F} = 0.030$ g/g, $K_{WSF} = 0.0525$ g/g, and $s = 11$. Using eq. (3a), in conjunction with eqs. (5) and (12), the NaCl-loaded film data could be fitted satisfactorily by setting $K_{W3} = 26.3$ g/g, as illustrated in Figure 1.

Sorption properties of solute

The reproducibility of the equilibrium sorption data obtained by the procedure described in Experimental is illustrated by the examples given in Table I. The said data are given in terms of two different partition (or distribution) coefficients, namely $K_P = C'_{NS}/c_{NS}$ (where $C'_{NS} = C_{NS}$ in g/cm^3 of hydrated film) and k_s previously defined in eq. (8). Values of K_P are given to facilitate comparison with data for this system reported by others[8–10] in this form. Agreement with such other data is satisfactory.

Reference to eq. (8) shows that k_s represents the ratio of the concentration of sorbed solute per unit volume of sorbed water to that in the external aqueous solution. Hence, if the polymer is relatively inert to solute and the imbibed water forms a true aqueous phase therein, in which the sorbed solute is dissolved, we expect $k_s = 1$. This condition is approached in highly

TABLE I
Water Content and Solute Partition and Diffusion Coefficients in Films of Normal Degree of Hydration C_W^0 (K_P in g cm^{-3} of Hydrated Film/g cm^{-3} of Aqueous Solution)

External NaCl solution concentration c_{NS} (g/cm^3)	K_P	k_s	C_{W0} (g/g)	C_W^0 (g/g)	NaCl content (mg/g)	$D_N \times 10^9$ (cm^2/s)
0.05	0.0357	0.224	0.139	0.145	1.54	1.0
	0.0315	0.198	0.140	0.142	1.41	0.8
	0.0392	0.240	0.147	0.153	1.72	1.1
	0.0336	0.186	0.153	0.155	1.50	1.5[a]
0.12	0.0460	0.276	0.145	0.154	4.85	1.3
	0.0450	0.274	0.140	0.145	4.80	1.1
	0.0385	0.223	0.146	0.150	4.10	1.2[a]
0.25	0.0430	0.340	0.102	0.158	9.17	—
	0.0524	0.367	0.113	0.168	11.33	(4.7)
	0.0519	0.363	0.112	0.164	11.18	(4.0)
	0.0417	0.322	0.100	0.156	8.91	(4.1)
	0.0503	0.365	0.108	0.158	10.84	(3.1)

[a] Film thickness in these two cases was 300 μm, whereas in all other cases it was 120 μm.

hydrated (hydrophilic) polymer matrices, but k_s would be expected to decline progressively, as the degree of hydration of the polymer decreases and water molecules are increasingly dispersed therein.[3,8,9] The values of k_s shown in Table I are, thus, in keeping with the low concentrations of imbibed water C_W^0 in the fully hydrated neat polymer (i.e., in the neat polymer equilibrated with pure water), which are also given in Table I. (Note also that the solute used here, being an electrolyte, is itself subject to dielectric exclusion from the matrix phase[11]; see also below). Also given therein are the concentrations of imbibed water C_{W0} attained upon equilibration with the respective NaCl solutions, which also represent the initial concentrations of imbibed water in the corresponding solute release experiments. The tendency of the C_{W0} values to be lower than those of C_W^0, which is clearly manifested in the data pertaining to the highest NaCl load, reflects the corresponding depression of water activity in the equilibrating salt solutions (a_W = 0.98, 0.95, and 0.83 for c_{NS} = 0.05, 0.12, and 0.25 g/cm^3, respectively).

Some, not previously reported, aging phenomena were observed, upon successive equilibration-elution cycles of the same film sample with NaCl solutions of the same concentration. No doubt, this is another manifestation of the slow structural relaxation, which was responsible for the protracted approach to equilibrium noted in our preceding study of water absorption kinetics.[2] Accordingly, these effects were examined in some detail. Examples of the results obtained are shown in Table II. To magnify the aging effect, the films used for this purpose were dried before the first equilibration-elution cycle. This is undoubtedly the reason for the unusually low K_P and C_{W0} values resulting from the first equilibration at the highest NaCl concentration. The conclusions which can be drawn from Table II are that (1) K_P and C_{W0} are not materially affected by the aforesaid cycling treatment at low NaCl concentrations; but (2) tend to rise significantly at high NaCl concentrations; nevertheless, (3) the magnitude and time scale of these effects are such that they may influence significantly the initial and final states of the system but not the course of the elution process.

TABLE II
Effect of Successive Equilibration and Elution Cycles on Sorption Parameters (units of K_P as in Table I)

Film no.	Equilibration sequence	c_{NS} (g/cm^3)	K_P	k_s	C_{W0} (g/g)	C_W^0 (g/g)
1	1st	0.05	0.0375	0.225	0.144	0.150
	3rd	0.05	0.0384	0.226	0.151	0.158
2	1st	0.12	0.0324	0.234	0.120	0.145
	2nd	0.12	0.0378	0.258	0.136	0.148
	3rd	0.12	0.0467	0.280	0.142	0.158
3	1st	0.25	0.0303	0.282	0.087	0.169
	2nd	0.25	0.0529	0.367	0.114	0.180
	3rd	0.25	0.0766	0.445	0.134	0.184

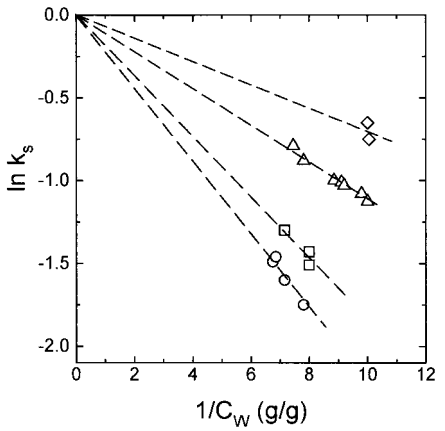

Figure 2 Dependence of the distribution coefficient k_s of NaCl on the concentration of imbibed water C_W, according to eq. (13), in CA films equilibrated with various NaCl solutions: c_{NS} = 0.05 (○), 0.12 (□), 0.25 (△) g/cm^3 or saturated solution (◇).

More detailed examination of Table I reveals a distinct tendency of K_P, k_s to increase with salt concentration, in keeping with the experimental findings of others[8,10] and with the theory of both Donnan and/or dielectric exclusion of electrolytes from charged and/or hydrophobic polymeric films, respectively. The expected tendency of K_P, k_s to increase with rising C_{W0}, at constant c_{NS}, is also clearly shown in Table II. As proposed in ref. 3 and subsequently demonstrated with the aid of experimental data in ref. 12 (see Fig. 4 therein), the aforesaid dependence is well described by

$$k_s = \exp(-\beta_{NS}/C_W) \tag{13}$$

where β_{NS} is a coefficient independent of C_W. The present data provide a fuller picture of the above behavior (see Fig. 2) and show that β_{NS} is a linear function of the concentration of the equilibrating solution (see Fig. 3); in particular,

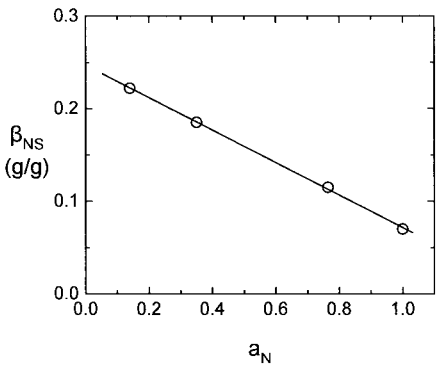

Figure 3 Dependence of the parameter β_{NS} in eq. (13) on the fractional saturation of the equilibrating NaCl solution (a_N).

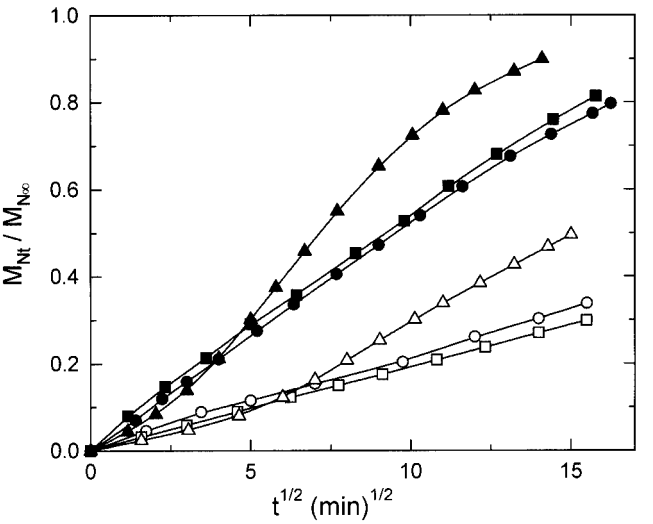

Figure 4 Typical kinetic curves of NaCl elution from CA films of thickness 120 (●, ■, ▲) or 300 (○, □, △) μm preequilibrated in NaCl solutions of concentration c_{NS} = 0.05 (●, ○), 0.12 (■, □), 0.25 (▲, △) g/cm^3.

$$\beta_{NS} = \beta_{NS1}(1 + \beta_{NS2}a_N) \tag{14}$$

where β_{NS1} = 0.247 g/g and β_{NS2} = −0.72.

Diffusion properties of solute

The diffusivity D_N of solute in the normally hydrated polymer matrix was measured by the well-established method of desorption (elution) into water, which is experimentally both more accurate and more convenient than absorption from aqueous solution.[12,13] Film samples preequilibrated with 0.05, 0.12, or 0.25 g/cm^3 NaCl solutions were used. Representative elution curves, plotted in the form of fractional amount eluted ($M_{Nt}/M_{N\infty}$) versus $\sqrt{t}$, are given in Figure 4. The initial linear portion of the curves pertaining to the lower preequilibration concentrations, in conjunction with the satisfactory agreement shown between thinner and thicker film data, indicates good conformity to Fickian kinetics. Values of the diffusion coefficient D_{NE} (see examples in Table I) were calculated from the slope of the initial linear portion of the experimental curves, according to the well known equation,

$$M_{Nt}/M_{N\infty} = 2(D_N t/\pi l^2)^{1/2} \tag{15}$$

On the other hand, the corresponding elution curves pertaining to the highest preequilibration concentration were S-shaped, indicating substantial deviations from Fickian kinetics (presumably attributable to the occurrence of substantial influx of water[3]; which is not appreciable at the lower preequilibrating concentrations considered above, due to the corresponding small differences in water activity between pre-

TABLE III
Partition Coefficients (K_P) and Diffusion Coefficients (D) of Na^+ and Cl^- in Films of Normal Degree of Hydration (units of K_P as in Table I)

	K_P		$D \times 10^9$ (cm^2/s)	
c_{NS} (g/cm^3)	Na^+	Cl^-	Na^+	Cl^-
0.05	0.0383	0.0363		
	0.0358	0.0368	1.0	3.2
	0.0407	0.0406	1.3	
0.12	0.0546	0.0565		
	0.0550	0.0579	1.2	3.0
	0.0493	0.0504		
0.25	0.0586	0.0636		
	0.0600	0.0656	0.9	1.4
	0.0600	0.0639		1.7

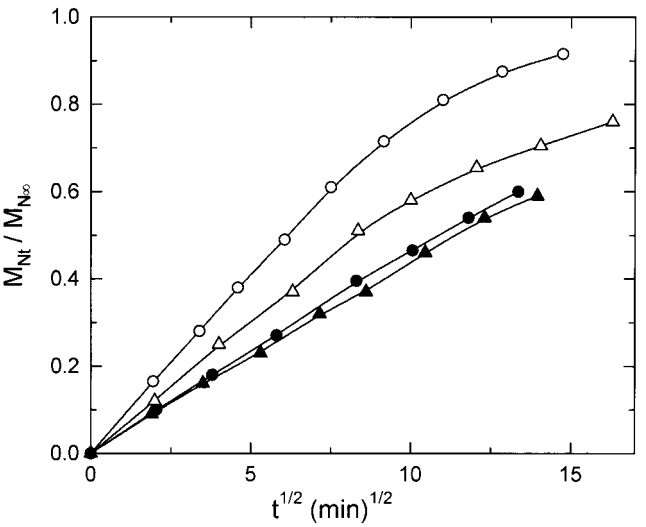

Figure 5 Desorption of Na-22 (●, ▲) or Cl-36 (○, △) tracers from films (120 μm thick) preequilibrated in active NaCl solutions of concentration 0.05 (○, ●) or 0.25 (△, ▲) g/cm^3 and then immersed in inactive solutions of the same concentration.

equilibrating and eluting baths in those cases). Accordingly, the D_N estimates obtained from the middle quasilinear portion of the elution curves (on the basis of eq. 15), and shown in parentheses in Table I, cannot be taken at face value. This leaves open the question of whether D_N does really increase (or, in general, change) materially at higher NaCl concentrations. To settle this point, experiments with radiotracers were performed, in which salt concentration, and hence water activity, was the same in equilibrating and eluting baths.

Ionic sorption and diffusion at constant salt concentration by use of tracers

The results of equilibrium sorption and elution experiments at constant NaCl concentration using Na-22 or Cl-36 as tracers (as described in Experimental) are reported in Table III. In the range of concentrations studied (c_{NS} = 0.05–0.25 g/cm^3), no material differences between cation and anion partition coefficients (K_P) are noticeable, indicating absence of substantial Donnan exclusion effects (from the small amount of carboxyl groups usually present in CA), as has also been reported by others.[10] The tendency of K_P for both ions to increase with salt concentration is in keeping with the results for NaCl reported in Table I and with the dielectric exclusion mechanism[11] referred to above.

The results of the corresponding elution experiments are shown in Figure 5. It can be seen that, under the conditions of undisturbed equilibrium maintained here between polymeric matrix and eluting bath, the elution curves of both ions do (as anticipated above) conform to Fickian kinetics at the highest salt concentration as well. The relevant diffusivity values (shown in Table III) are in keeping with those for NaCl given in Table I at the lower salt concentrations (bearing in mind that salt diffusivity is controlled by that of the slower ion). They also show that no useful diffusivity values can be extracted from the non-Fickian NaCl curves obtained at the highest salt concentration; in fact, it appears that D_N tends to decline (rather than increase as suggested by the values in parentheses in Table I) under these conditions (presumably as a result of reduced degree of hydration of the matrix).

The aforementioned results are of general interest, because they bring to light the need to check for, and guard against, osmotic effects, when measuring solute diffusivities in hydrated polymers by the above method of solute desorption.

On the basis of the sum total of our diffusion data, mean values of D_{NE} = 1.0–2.2 $\times 10^{-9}$ cm^2/s (considered to be essentially independent of solute concentration) were determined for C_W^0 = 0.15–0.17 g/g, respectively, which agree well with those calculated by eq. (10), using the diffusion coefficient of NaCl in aqueous solution,[14] $D_{NS} = 1.6 \times 10^{-5}$ cm^2/s, and the

TABLE IV
Dependence of D_N on the Degree of Hydration of the CA Film as Measured Experimentally and as Calculated by eq. (10) with Parameter Values as Specified in the Text

C_W^0 (g/g)	$D_N \times 10^9$ cm^2/s (experimental)	$D_N \times 10^9$ cm^2/s (calculated)
0.142	0.8	0.73
0.150	1.0	1.08
0.153	1.2	1.25
0.155	1.5	1.37
0.160	1.8	1.71
0.168	2.2	2.39

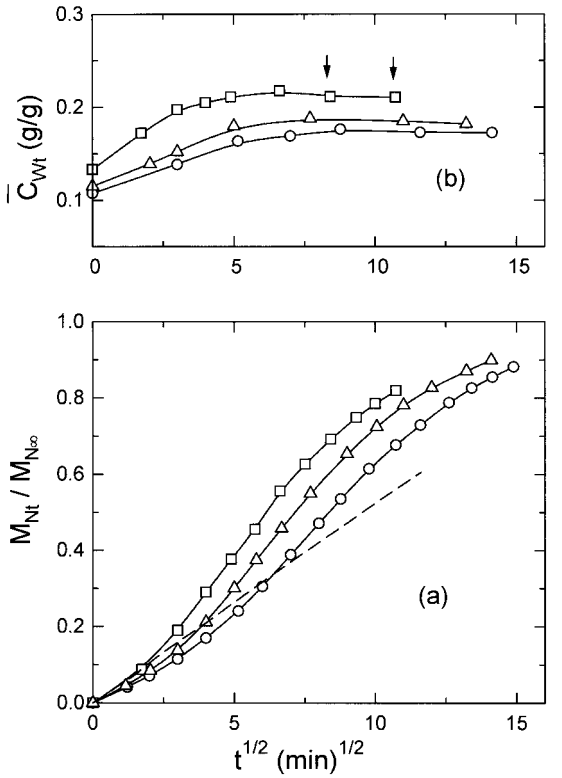

Figure 6 (a) Elution of NaCl from three CA films preequilibrated in concentrated NaCl solutions (c_{NS} = 0.25 g/cm^3) with resulting NaCl load in the film 0.0108 (○), 0.0112 (△), or 0.0169 (□) g/g of dry polymer. Film thickness: 120 μm. Degree of hydration of the films: C_W^0 = 0.158 (○), 0.164 (△), or 0.175 (□) g/g. The broken line represents the initial part of an elution curve typical of films preequilibrated in dilute NaCl solutions. (b) Concurrent variation of mean concentration of imbibed water in the aforementioned films. For the meaning of the arrows see inset of Fig. 7.

parameters previously established,[12] namely, B_{N1} = 1.92 g/g, B_{N2} = 0.05 g/g (see Table IV).

Concurrent solute release and solvent sorption kinetics

The results reported above show clearly that water sorption plays an important role in determining solute release kinetics from films loaded with substantial amounts of (dissolved) solute. Accordingly, it is important, in such cases, to monitor the variation of the concentration of imbibed water $\bar{C}_{Wt}$ during the elution experiment. This was done for films preequilibrated with 0.25 g/cm^3 NaCl solutions by the method described in Experimental. Typical results are shown in Figure 6.

As previously mentioned, the prominent S-shape of the experimental M_{Nt} versus $\sqrt{t}$ elution curves [see Fig. 6(a)] reflects an acceleration of the elution process, caused by an increase in D_N attributable to influx of water into the film, driven by the difference in activity a_W between imbibed water and eluting bath (and further enhanced by the relaxation process B observed in Part I).

On the other hand, the measured $\bar{C}_{Wt}$ [see Fig. 6(b)] first rises (as a result of the osmotic action of the solute) well beyond the value C_W^0 corresponding to full hydration of the neat film, reaches a maximum, and then begins to decline as the matrix is depleted of solute.[3,12,15–18] However, the said decline is very slow and $\bar{C}_{Wt}$ returns to C_W^0 only long after complete elution of the solute. Hence, this deswelling process may be assumed to represent, at least in a large part, a slow structural relaxation, similar to that (governed by relaxation frequency β_{WC}), which controls the slow approach to equilibrium during water absorption by neat CA film.[2] Indeed, kinetic analysis of the rate of decline of $\bar{C}_{Wt}$ in the solute-depleted matrix showed good conformity to first-order relaxation kinetics (represented by the solid line in Fig. 7), namely,

$$\frac{d\bar{C}_{Wt}}{dt} = \beta_{WD}(C_W^0 - \bar{C}_{Wt}) \tag{16}$$

and yielded a relaxation frequency β_{WD} = 3–6 × 10^{-6} s^{-1} (i.e., ca. one order of magnitude lower than β_{WC}).

Detailed computer simulation of the combined solvent–sorption and solute–release kinetic behavior is discussed below.

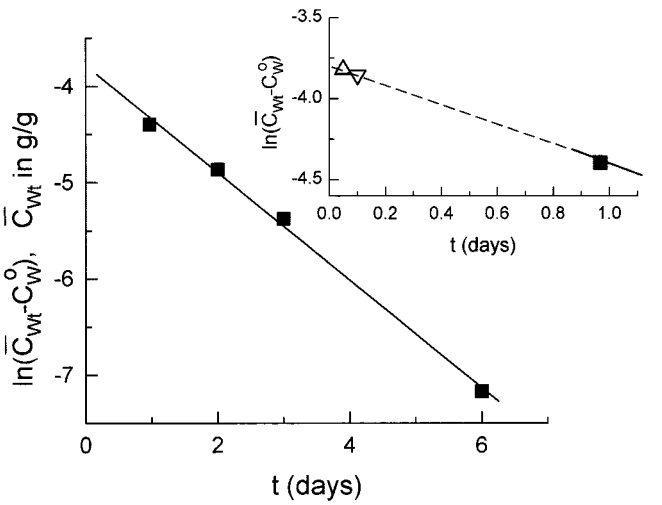

Figure 7 Linear first-order plot, according to eq. (16), of the late time portion of the uppermost curve of Fig. 6(b), corresponding to deswelling of the polymeric matrix after complete elution of solute (the line drawn through the experimental points corresponds to β_{WD} = 6 × 10^{-6} s^{-1}). Inset: The broken line represents back extrapolation (on an expanded time scale) of the solid line shown in the main figure through earlier experimental points [marked by arrows in Fig. 6(b)] corresponding to incomplete elution of solute. Fractional amounts of remaining solute: 0.31 (△); 0.18 (▽); 0.00 (■).

Computer simulation results

Computer simulation of concurrent solute release and water uptake kinetics was performed, on the basis of the model presented in the theoretical section, under the boundary conditions prevailing in the high-solute-load elution experiments, as given by eqs. (2) with C_{W0} = 0.112 g/g (a_{W0} = 0.83) and C_{N0} = 0.0114 g/g (a_{N0} = 0.78).

The relevant input sorption and diffusion model parameters were determined from the results of (1) the independent experimental measurements reported above and (2) the preceding study of the kinetics of liquid water absorption by neat CA film.[2]

The presence of osmotically active solute is represented in the model by endowing the matrix with excess sorptive, or (equivalently) swelling, capacity [represented by eq. (5)]; which is, however, subject to continuous decline, during the elution experiment, as the matrix is progressively depleted of solute. Nevertheless, water uptake is sufficiently fast by comparison with elution (as indicated by the values of the dimensionless indices defined in ref. 1: $D_{NE}/D_W \sim 10^{-2}$, $l^2\beta_{WB}/D_{NE} \sim 10^2$) to ensure that swelling of the matrix can continue well past the point corresponding to the fully hydrated neat film, before it is overtaken by the aforesaid continuing drop in excess swelling capacity, at which stage the water absorption phase is brought to an end.

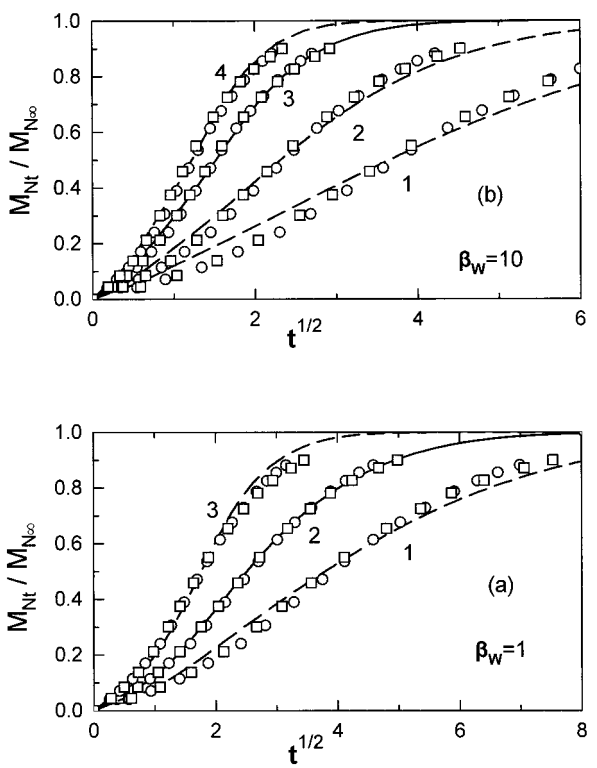

Figure 8 Comparison of dimensionless simulated NaCl elution kinetic curves (defined by lines) computed using (a) $\boldsymbol{\beta_{WB}}$ = 1 or (b) $\boldsymbol{\beta_{WB}}$ = 10 and $\mathbf{D_{NS}}$ = 100 (curves 1), 300 (curves 2), 1000 (curves 3), 2000 (curve 4) (other parameters as given in the text), with experimental data derived from two CA films of C_W^0 = 0.16 g/g (□, ○), replotted each time on a dimensionless time scale $D_{WB}t/l^2$, where D_{WB} is chosen for best superposition on the relevant simulated curve. The resulting D_{WB} values are given in Table V. Best fit is symbolized by solid lines.

TABLE V
Experimental Values of D_W (D_{WB}) Estimated by Comparison of Experimental NaCl Elution Data with Simulated Curves Computed for Various Values of $\mathbf{D_{NS}}$ (for given $\boldsymbol{\beta_{WB}}$) and Resulting Calculated Values of the Aqueous Diffusivity of NaCl (D_{NS} = $\mathbf{D_{NS}}D_{WB}$)

C_W^0 (g/g)	$\boldsymbol{\beta_{WB}}$	$\mathbf{D_{NS}}$	$D_{WB} \times 10^7$ (cm²/s)	$D_{NS} \times 10^5$ (cm²/s) calculated
0.16	1	100	1.3	1.3
		250	0.67	1.7
		300	0.61	1.8
		1000	0.25	2.5
	10	100	1.2	1.2
		300	0.48	1.4
		1000	0.20	2.0
		2000	0.13	2.6

This phase was simulated by adopting the range of input parameter values shown in Part I[2] to be adequate for the simulation of the kinetics of water absorption by neat film; except for the fact that there is here no fixed ultimate absorption equilibrium to be reached and, in any case, there is no time for the slow relaxation C to play a significant role in any way. Accordingly, input values of $\boldsymbol{\beta_{WB}}$ = 1–10 were used as in Part I[2] (with $\alpha_A = K_{WI}/K_{WF}$ = 0.3, $\alpha_B = K_{WB}/K_{WF}$ = 0.7, α_C = 0), assuming the dependence of a_W on C_W and C_N to be given correctly by eqs. (3), (5), and (12) over the whole region $a_{W0} \leq a_W \leq 1$. (Note that no input value for D_W was used.)

In view of the fact that no prior independent guidance was obtainable as to what quantitative formulation of the combined osmotic-cum-relaxation behavior should be assumed during the ensuing desorption phase, two extreme possibilities were considered.

The first extreme possibility is that osmotically induced swelling is relatively easily recoverable; hence, deswelling will tend to follow the aforementioned continuous drop in excess swelling capacity brought about by the elution of solute.[1] In view of the relaxation behavior revealed by the kinetic analysis of Fig. 7, β_{WB} was replaced by β_{WD}.

Dimensionless simulated solute release curves were computed on this basis for a series of $\mathbf{D_{NS}} = D_{NS}/D_W$ values. Fitting to the experimental curves was effected (as in Part I) by replotting the experimental data on the dimensionless time scale $D_{WB}t/l^2$, where D_{WB} represents the experimental value of D_W, which produces optimum superposition of experimental and simulated curves. Examples of the results obtained from

computations based on $\boldsymbol{\beta}_{\mathbf{WB}} = 1$ or $\boldsymbol{\beta}_{\mathbf{WB}} = 10$ (with $\boldsymbol{\beta}_{\mathbf{WD}} = 0.001$) are shown in Figure 8(a, b), respectively. The pertinent D_{WB} values are given in Table V.

The physical meaningfulness and validity of these results is subject to rather exacting checks. In particular, one should bear in mind that (1) there is only one parameter ($\mathbf{D}_{\mathbf{NS}}$) which can be manipulated to simulate the detailed shape of the full elution curve and (2) the chosen $\mathbf{D}_{\mathbf{NS}}$ value (in conjunction with the resulting D_{WB}) should be consistent with the known diffusivity of NaCl in aqueous solution ($D_{NS} = 1.6 \times 10^{-5}$ cm^2/s).[14] The pertinent calculated values $D_{NS} = \mathbf{D}_{\mathbf{NS}} D_{WB}$ are given in column 5 of Table V. On this basis, one can see that excellent results were achieved with $\boldsymbol{\beta}_{\mathbf{WB}} = 1$ and $\mathbf{D}_{\mathbf{NS}} \cong 300$ [cf. solid line in Fig. 8(a) and corresponding calculated D_{NS} in Table V]. The results obtained for $\boldsymbol{\beta}_{\mathbf{WB}} = 10$ are clearly much less satisfactory in this respect [as shown in Fig. 8(b) and Table V].

Another very important check is that the optimum value of D_{WB} (D^0_{WB}), derived from the elution data as above, should also produce a good fit to the observed concomitant variation of the water content of the film. Pertinent examples [corresponding to the elution curves of Fig. 8(a, b), respectively] are given in Figure 9(a, b). Here, a reasonably good fit of the data for the absorption phase can again be achieved only by the input values $\boldsymbol{\beta}_{\mathbf{WB}} = 1$, $\mathbf{D}_{\mathbf{NS}} \cong 300$. It is noteworthy that the results obtained in Part I for water absorption by neat CA film are also consistent with $\boldsymbol{\beta}_{\mathbf{WB}} = 1$ in preference to $\boldsymbol{\beta}_{\mathbf{WB}} = 10$; furthermore, the corresponding D^0_{WB} ($\approx 0.7 \times 10^{-7}$ cm^2/s, see Table V) also matches the experimental value of D_W (denoted by D^0_{WA}) determined in Part I for analogous boundary conditions ($a_{W0} = 0.85$, see Table I of Part I). This agreement means that, given the values of D^0_{WA} and of the non-Fickian water uptake parameters determined in Part I, the present model can predict satisfactorily the rate and kinetics of both solute release and concomitant water sorption, during the water absorption phase.

On the other hand, Figure 9 shows clearly that the modeling approach to the water desorption phase tried above consistently overestimates the amount of imbibed water which is lost during the earlier stages of the desorption process. The concentration profiles of imbibed water [$\mathbf{C}_{\mathbf{W}}(\mathbf{x}, \mathbf{t})$] and solute [$\mathbf{C}_{\mathbf{N}}(\mathbf{x}, \mathbf{t})$], as well as of the corresponding water activity [$a_W(\mathbf{x}, \mathbf{t})$], for the case of $\boldsymbol{\beta}_{\mathbf{WB}} = 1$, $\mathbf{D}_{\mathbf{NS}} = 300$, are shown in Figure 10. It is clear that the rate of water transport is sufficiently high for diffusion equilibrium [i.e., $a_W(\mathbf{x}, \mathbf{t}) \cong 1$] to be attained by the end of the water absorption phase [cf., Fig. 10(a, b)] and to be maintained thereafter. It follows that, during the desorption phase, one is really observing the kinetics of relaxation controlled deswelling, and the deswelling process is much less influenced by the osmotic effect than was assumed above.

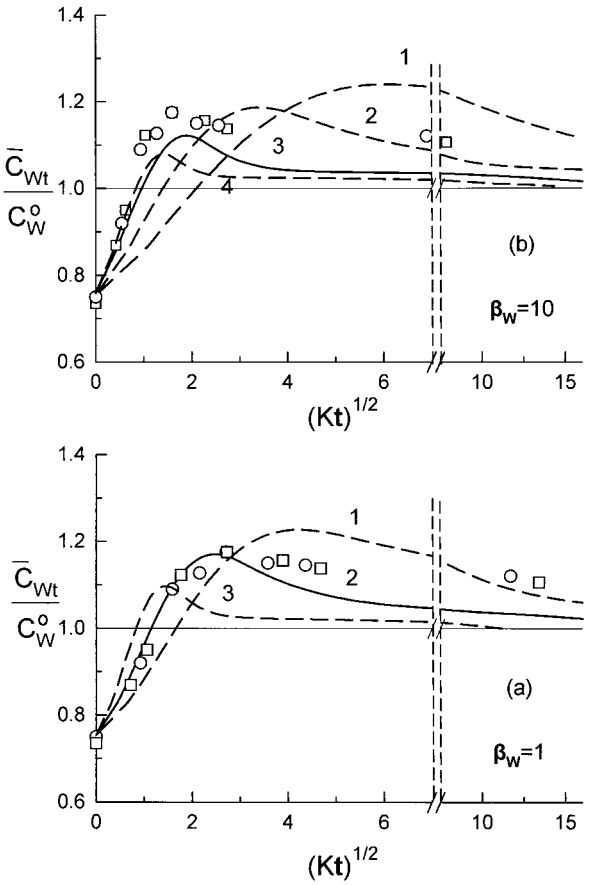

Figure 9 Display of the experimental (○, □) and simulated (curves 1–4) dimensionless plots of the water content of the CA matrix ($\bar{C}_{Wt}$), which correspond to the NaCl elution and pertinent simulation plots shown in Figure 8, using the same symbolism as in Figure 8. For the sake of maintaining clarity in the figure, the experimental data are plotted on the dimensionless time scale $D^0_{WB}t/l^2$ (where D^0_{WB} is the value of D_W which best fits the relevant NaCl elution data of Fig. 8) and comparison with the simulated curves is effected by plotting the latter on a scale $KD^0_{WB}t/l^2$, where $K = D_{WB}/D^0_{WB}$: (a) $\boldsymbol{\beta}_{\mathbf{WB}} = 1$; $D^0_{WB} = 0.61 \times 10^{-7}$ cm^2/s; $K = 2.2$ (curve 1), 1 (curve 2), 0.42 (curve 3); (b) $\boldsymbol{\beta}_{\mathbf{WB}} = 10$; $D^0_{WB} = 0.20 \times 10^{-7}$ cm^2/s; $K = 6.0$ (curve 1), 2.4 (curve 2), 1 (curve 3), 0.65 (curve 4). It is shown that D^0_{WB} for the case of $\boldsymbol{\beta}_{\mathbf{WB}} = 1$ yields a good fit to the $\bar{C}_{Wt}$ data, during the water absorption phase. Failure to fit the data beyond this point is due to the fact that deswelling is controlled by a different mechanism (see text and Fig. 11).

These findings prompt consideration of the other extreme possibility of modeling the water desorption phase referred to above. This involves the assumption that the osmotically induced excess swelling achieved during the water absorption phase is semi-permanent and (in analogy with mechanically induced deformation beyond elastic limits) the polymeric matrix can relax from this expanded (superhydrated) state to its normal state of hydration at a rate which is both very

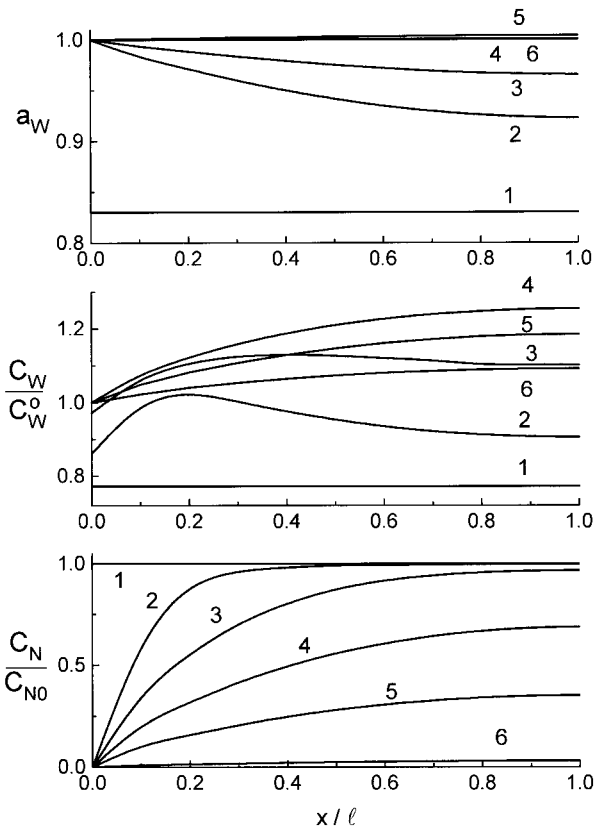

Figure 10 Computed distribution of water activity and of normalized water (C_W/C_W^0) and NaCl (C_N/C_{N0}) concentrations across the CA film (from the exposed surface at $x = 0$ to the midplane at $x = l$) at various stages of the elution process simulated by curve 2 of Figure 8(a), corresponding to fractional amounts of eluted solute: $M_{Nt}/M_{N\infty} = 0$ (line 1), 0.107 (line 2), 0.244 (line 3), 0.505 (line 4), 0.750 (line 5), 0.978 (line 6).

slow and insensitive to the minor changes in osmotic driving force resulting from elution of the remaining solute. On this basis, calculation of $C_W(x, t)$, and hence of $\bar{C}_{Wt}$, during the water desorption phase, simplifies to application of the equivalent of eq. (16) at each x, t [with $a_W(x, t) = 1$]. The results obtained for the case of $\boldsymbol{\beta_{WB}} = 1$, $\mathbf{D_{NS}} = 300$ are shown in Figure 11. It can be seen that the new computed $\bar{C}_{Wt}$ desorption line tends to underestimate somewhat the amount of water lost but otherwise simulates the observed kinetic behavior very closely. (On the other hand, the effect on the corresponding solute elution curve is clearly too small to affect the validity of our previously drawn conclusions in any way). The insensitivity of the relaxation process to C_{NS} was confirmed by back extrapolation of the first-order plot, which was shown in Fig. 7 to provide an adequate representation of the relaxation-controlled deswelling of the solute-depleted matrix. The inset of that figure shows that the same plot also applies to earlier stages of the said deswelling process (where the matrix still contains substantial amounts of solute), up to a point remarkably close to the maximum of the $\bar{C}_{Wt}$ curve [as illustrated by the points marked with arrows in Fig. 6(b)].

CONCLUSIONS

We have reported and discussed above the results of a combined experimental and computer simulation study of the performance of a model monolithic controlled release device, consisting of a CA matrix (in the form of a thin film) loaded with a substantial amount of NaCl (representing a realistic load of osmotically active solute) and activated by water as solvent. To ensure perfectly uniform distribution of the load of solute, the latter was introduced by prior equilibration of the CA film with a concentrated NaCl solution. A significant feature of this study was the fact that both solute release and the accompanying variation of the total water content (and hence the degree of swelling) of the CA matrix were measured and simulated, thus providing a more extensive and exacting test for the underlying theoretical model presented in the theoretical section.

The results obtained indicated that the solute release process exhibited substantial deviation from Fickian kinetics, in the form of a markedly S-shaped release curve when plotted on a $\sqrt{t}$ basis (in contrast to the Fickian behavior observed in the case of small solute loads). At the same time, the water content of the CA matrix $\bar{C}_{Wt}$ was observed to rise, as a result of the osmotically enhanced absorption of water, well past the value corresponding to the fully hydrated neat matrix C_W^0, before a very slow decline back to C_W^0 (extending well beyond the completion of the release

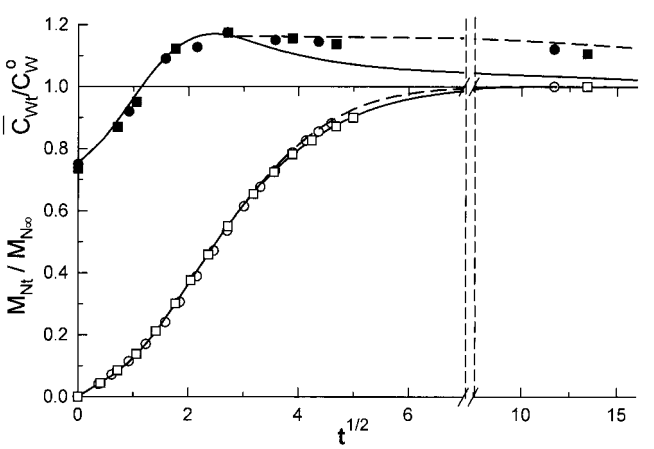

Figure 11 Experimental (points) and simulated (lines) kinetics of solute release (open points) and attendant variation of the water content (filled points) of the CA matrix [corresponding to curves 2 in Figs. 8(a) and 9(a), respectively], showing the difference which arises in simulated kinetics during the desorption phase, when the deswelling process is assumed to be primarily osmotically driven (solid lines) or fully relaxation-dependent (broken lines).

process) had begun. This protracted desorption process was shown to be controlled by a long-term structural deswelling relaxation, insensitive to osmotic effects due to remnants of unreleased solute. Accordingly, it could be adequately simulated in terms of simple relaxation kinetics, using a relaxation frequency determined from deswelling of pure polymer.

On the other hand, solute release over the whole experimental range, as well as the concomitant variation of $\bar{C}_{Wt}$ during the critical water absorption phase, were simulated with a high degree of success, using the model presented in the theoretical section. The latter was parameterized on the basis of the information derived from independent studies of solvent and solute sorption and diffusion properties reported in Part I[2] and in Experimental of the present article. The strategy followed was to compare simulated (dimensionless) release curves, for a series of $\mathbf{D_{NS}} = D_{NS}/D_W$ values, with the relevant experimental data plotted in the form $M_{Nt}/M_{N\infty}$ versus $D_{WB}t/l^2$, where D_{WB} represents in each case the experimental value of D_W, which produces optimum superposition of experimental to the corresponding simulated curve. The first successful test of the theoretical model was that the value of $\mathbf{D_{NS}}$, which produced a simulated curve coincident with the experimental one over the whole experimental range also yielded a D_{WB} consistent with the known value of the diffusion coefficient of NaCl in aqueous solution D_{NS} ($=\mathbf{D_{NS}}D_{WB}$). A second no less demanding check was that the same D_{WB} value (denoted by D^0_{WB}) had to produce a good fit of the corresponding experimental and simulated water absorption curves. It is also remarkable that D^0_{WB} matched the corresponding value D^0_{WA}, determined in Part I[2] for water absorption in neat CA under similar boundary conditions ($a_{W0} = 0.83$), and that the optimum values of the non-Fickian parameters α_A and β_{WB} estimated in Part I were confirmed here. This means that the model presented here has been shown to be capable of providing reliable prediction of the rate and kinetics of both (osmotically active) solute release and (non-Fickian) solvent sorption processes, on the basis of independently derived information relating to solvent and solute sorption and diffusion properties and to the relaxation behavior of the polymer matrix.

The results reported above constitute a good example of the practical applicability of our modeling work and of the possibility of using computer simulation as an important tool for the rational design of monolithic controlled release devices exhibiting complex kinetic behavior.

This work was performed in the framework of the Program "Excellence in the Research Institutes" financed by the General Secretariat for Research and Technology, Ministry of Development, Athens, Greece and the European Union.

References

1. Papadokostaki, K. G.; Polishchuk, A. Ya.; Petrou, J. K. J Polym Sci, Part B: Polym Phys 2002, 40, 1171.
2. Papadokostaki, K. G.; Petrou, J. K. J Appl Polym Sci, accepted.
3. Petropoulos, J. H.; Papadokostaki, K. G.; Amarantos, S. G. J Polym Sci, Part B: Polym Phys 1992, 30, 717.
4. Polishchuk, A. Ya.; Zaikov, G. E.; Zimina, L. A.; Petropoulos, Ya. I.; Lobo, V. M. M. Chem Phys Rep 1997, 16, 311.
5. Yasuda, H.; Lamaze, C. E.; Peterlin, A. J Polym Sci, A2 1971, 9, 1117.
6. Crank, J. The Mathematics of Diffusion, 2nd ed.; Clarendon Press: Oxford, UK, 1975; Chapter 4.
7. Apicella, A.; Hopfenberg, H. B. J Appl Polym Sci 1982, 27, 1139.
8. Taniguchi, Y.; Horigome, S. J Appl Polym Sci 1975, 19, 2743.
9. Lonsdale, H. K.; Merten, U.; Riley, R. L. J Appl Polym Sci 1965, 13, 1341.
10. Heyde, M. E.; Peters, C. R.; Anderson, J. E. J Colloid Interface Sci 1975, 50, 467.
11. Glueckauf, E. Desalination 1976, 18, 155.
12. Papadokostaki, K. G.; Petropoulos, J. H.; Amarantos, S. G. J Appl Polym Sci 1998, 69, 1275.
13. Yasuda, H.; Lamaze, C. E. J Appl Polym Sci 1969, 13, 2209.
14. Horvath, A. L. Handbook of Electrolyte Solutions; Ellis Horwood: West Sussex, UK, 1985.
15. Polishchuk, A. Ya.; Zaikov, G. E. Multicomponent Transport in Polymer Systems for Controlled Release; Gordon and Breach: New York, 1997; pp. 89–91.
16. Brown, D.; Bae, Y. H.; Kim, S. W. Macromolecules 1994, 27, 4952.
17. Lee, P. I.; Kim, C.-J. J Controlled Release 1991, 16, 229.
18. Bae, Y. H.; Okano, T.; Ebert, C.; Heiber, S.; Dave, S.; Kim, S. W. J Controlled Release 1991, 16, 189.